

Coherent Cherenkov radiation as an intense THz source

V Bleko¹, P Karataev², A Konkov³, K Kruchinin², G Naumenko³,
A Potylitsyn³ and T Vaughan²

¹ RASA Center in Tomsk, Tomsk Polytechnic University, Lenin Ave. 30, Tomsk, 634050, Russian Federation

² John Adams Institute at Royal Holloway, University of London, Egham, TW20 0EX, UK

³ Tomsk Polytechnic University, Lenin Ave. 30, Tomsk, 634050, Russian Federation

E-mail: bleko_vitold@mail.ru

Abstract. Diffraction and Cherenkov radiation of relativistic electrons from a dielectric target has been proposed as mechanism for production of intense terahertz (THz) radiation. The use of an extremely short high-energy electron beam of a 4th generation light source (X-ray free electron laser) appears to be very promising. A moderate power from the electron beam can be extracted and converted into THz radiation with nearly zero absorption losses. The initial experiment on THz observation will be performed at CLARA/VELA FEL test facility in the UK to demonstrate the principle to a wider community and to develop the radiator prototype. In this paper, we present our theoretical predictions (based on the approach of polarization currents), which provides the basis for interpreting the future experimental measurements. We will also present our hardware design and discuss a plan of the future experiment.

1. Introduction

The THz frequency of electromagnetic radiation always ranges from 10 – 0.1 THz and corresponds to the wavelength range from 30 μm to 3 mm [1]. Due to its ability to excite interatomic oscillations in many substances, THz radiation has numerous practical applications from spectroscopy of chemical and biological objects to fulfilling military or civilian security purposes [2–4].

However, there are difficulties in developing efficient methods for generating coherent THz radiation. Modern methods used in optical and infrared regions are not applicable in this case [5]. To generate the radiation in the frequency range from 0.1 – 1.6 THz, Gunn diodes, GaAs based Schottky Barrier Diodes and Backward Wave Oscillators (BWO) are widely used. They provide a CW radiation with continuous frequency adjustment [6] and power of order of several microwatts for diodes to a few watts for BWOs. All above-mentioned devices are low power and narrowband, which are the main disadvantages of them. The high frequency range is covered by new quantum cascade laser technology and gas lasers emitting radiation from 1.6 to 2.5 THz. Typical optical to THz conversion is very low (about 10% for a single stage [7]). The output power falls from 1 Watt at 1 THz to below 0.1 Watt at 3 THz with even newer distributed or travelling photomixer designs [8]. One should pay particular attention to Free Electron Lasers [9,10], which, despite some of their obvious advantages, have a limited range of tasks because of their huge sizes.



As is generally known, when a relativistic charged particle passes by any non-uniform medium with a distance comparable to or shorter than the parameter $\gamma\lambda/2\pi$ (here γ is the charged particle Lorentz-factor and λ is the radiation wavelength), its field polarizes the medium atoms [11]. The excited atoms start oscillating (representing currents changing in time) and become sources of EM radiation. Depending on the geometry of the medium, it can be treated as diffraction radiation (DR) from a metal surface [12] or Cherenkov radiation (ChR) from a transparent medium. If the radiation wavelength is comparable to or longer than the bunch length, all electrons emit radiation more or less in time stimulating each other's emission. As a result the photon yield is proportional to the square of the number of particles in the bunch; in the other words, the radiation is emitted coherently [13].

DR is emitted whenever a uniformly and rectilinearly moving charge passes in the vicinity of an optical inhomogeneity (target) [14] with impact parameter, h (being the shortest distance between the target and the electron beam), satisfying the following condition:

$$h \leq \frac{\gamma\lambda}{2\pi}. \quad (1)$$

Assuming 14 GeV beam energy of the LCLS accelerator [9] and 1 THz (0.3 mm) frequency any inhomogeneity (different vacuum pipe diameter, flanges, viewports, etc.) paced within 1.3 m radius away from the beam will radiate at THz frequencies. An optimal radiator might extract a moderate power from the beam and convert it into a THz radiation beam for utilization by THz user community.

ChR is generated when a charged particle speed is higher than the speed of light inside a medium [15]. Its direction is determined by the following relation:

$$\cos \theta_{\text{Ch}} = \frac{v_{\text{light}}}{v_{\text{particle}}} = \frac{c/n}{c\beta} = \frac{1}{n\beta}. \quad (2)$$

However, the particle itself does not have to go through the substance. The energy loss due to ChR and DR is very small in comparison to the total power of the beam. Such generation geometry is very convenient. It excludes the ionization losses due to direct interaction with the target; and, therefore, it enables a parallel installation of several generating station for the same beam.

When generating ChR the particle also generates pure DR from all surfaces of the target. In [16–20] the authors have tried to unify the theory and merge different radiation types together. The method for the unified theory was called as polarization currents approach (PCA) [20]. It should be mentioned that the authors [21–24] have partially verified the model experimentally.

In this paper, we propose a scheme to generate intense THz radiation beams using the ChR mechanism at CLARA (Compact Linear Accelerator for Research and Application) facility in Daresbury Laboratory (UK) with intermediate energy of 50 MeV. The paper will review the theoretical background, overview the hardware status and experimental plans.

2. Theoretical background

In this paper we used polarization current method enabling us to calculate polarization radiation characteristics for conditions close to the experimental ones. The method is valid for description of polarization radiation generated by short charged particle bunches passing by a target with finite outer dimensions and known dielectric permittivity (see figure 1).

One should note that in such geometry ChR and DR will be generated simultaneously [21]. The DR intensity depends on the prism sides AC and CB (see figure 1), ChR is generated from the side AC . Changing the length of the side one may change the radiation intensity.

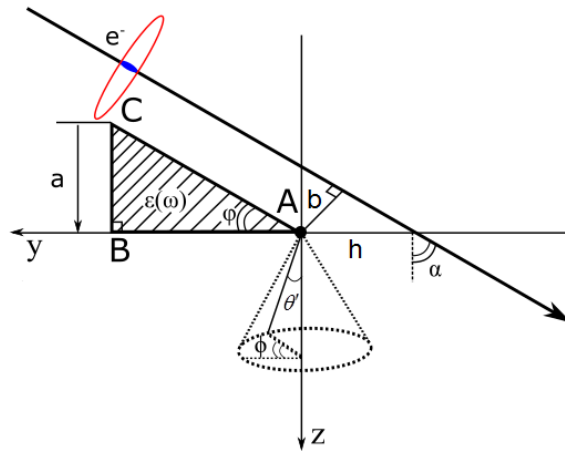


Figure 1. Scheme of polarization radiation generated by a charged particle moving rectilinearly in the vicinity of a dielectric prism.

To calculate the spectral-angular distribution of the ChR in vacuum we use the model derived in [19] (see the equation (16)):

$$\begin{aligned}
 \frac{d^2W}{d\omega d\Omega} = & \frac{e^2}{4\pi^2 c} \frac{\beta^2 \cos^2(\theta - \alpha)}{K^2 |P|^2} \left| \frac{\varepsilon(\omega) - 1}{\varepsilon(\omega)} \right|^2 \times \\
 & \left| 1 - \frac{P \exp\left(i \frac{\omega}{\beta c} a \coth \varphi\right) + \Sigma \coth \varphi \exp\left(-ia \frac{\omega}{\beta c} P\right)}{P + \Sigma \coth \varphi} \right|^2 \times \\
 & \frac{\exp\left[-2 \frac{\omega}{\gamma \beta c} (h + a \coth \varphi) K \cos \alpha\right]}{1 - \beta^2 \cos^2(\theta - \alpha) + \beta^2 \sin^2 \alpha (1 - \sin^2(\theta - \alpha) \sin^2 \phi) + 2\beta \sin \alpha \sin(\theta - \alpha) \cos \phi} \times \\
 & \left[\left| \frac{\varepsilon(\omega)}{\varepsilon(\omega) \cos(\theta - \alpha) + U} \right|^2 \left| \cos \alpha (\gamma^{-1} \sin(\theta - \alpha) - iKU \cos \phi) + \right. \right. \\
 & \left. \left. + \sin \alpha (iK \sin(\theta - \alpha) + \gamma^{-1}U \cos \phi) - \gamma \beta U \sin(\theta - \alpha) \sin^2 \phi \right|^2 + \right. \\
 & \left. \gamma^2 \sin^2 \phi \left| \frac{\sqrt{\varepsilon(\omega)}}{\cos(\theta - \alpha) + U} \right|^2 (\sin^2(\theta - \alpha) + |U|^2) \times \right. \\
 & \left. \left. [1 - \beta^2 \cos^2(\theta - \alpha) + 2\beta \gamma^{-2} \sin \alpha \sin(\theta - \alpha) \cos \phi - \gamma^{-2} \sin^2 \alpha (K^2 - \gamma^{-2})] \right]. \quad (3)
 \end{aligned}$$

where we used the following notations:

$$\begin{aligned}
 U &= \sqrt{\varepsilon(\omega) - \sin^2(\theta - \alpha)}, \\
 P &= \cos \alpha - \beta U + i\gamma^{-1}K \sin \alpha, \\
 \Sigma &= \sin \alpha + \beta \sin(\theta - \alpha) \cos \phi - i\gamma^{-1}K \cos \alpha, \\
 K &= \sqrt{1 + (\gamma \beta \sin(\theta - \alpha) \sin \phi)^2}.
 \end{aligned}$$

In this equation ω is the frequency of the emitted radiation; α is the charged particle incident angle; θ and ϕ are the polar and azimuthal observation angles respectively; a is the side BC

(see figure 1); $h = b/\cos\alpha$ is the impact parameter. The radiation angle θ is measured from the trajectory of a charged particle and is connected with the angle θ' that defined relative to the z -axis of the Cartesian coordinates system (see figure 1) by the simple relation: $\theta' = \theta - \alpha$.

The equation (3) takes into account both DR and ChR types. The following pole in the denominator is responsible for the ChR:

$$\left| \cos\alpha - \beta\sqrt{\varepsilon(\omega) - \sin^2(\theta - \alpha)} + i\gamma^{-1}K \sin\alpha \right| \rightarrow 0. \quad (4)$$

The equation (4) is somewhat different from classical relation (2), defining the direction of the ChR propagation. It should be noted that, when $\alpha \rightarrow 0$, the equation (4) coincides with classical Cherenkov radiation condition represented in vacuum.

The fact that the equation (3) contains poles responsible for ChR. It enables us to control the direction of the Cherenkov radiation photon yield by changing the prism angle φ in the range $0 < \varphi < \pi/2$. This aspect might significantly simplify an experimental setup eliminating the need to use additional optical elements for radiation focusing or extraction.

The spectral-angular distributions of polarization radiation appearing when a fast charged particle passes by parallel to the dielectric prism ($\alpha = \pi/4$) are illustrated in the figure 2. As a target a PTFE (Teflon) triangular prism with the opening angle of $\pi/2$ is used. The calculation parameters were chosen for the linear electron accelerator CLARA [25] and listed up in the table 1.

Table 1. CLARA beam parameters.

Beam Energy	55 MeV
Beam Charge	100 pC
r.m.s. Beam Size (x/y)	50/200 μm
Bunch Length (r.m.s.)	0.15 ps

ChR maximum intensity corresponds to the angle of $\theta_{\text{Ch}} = 43^\circ$ with respect to the particle trajectory determined by the equation (4).

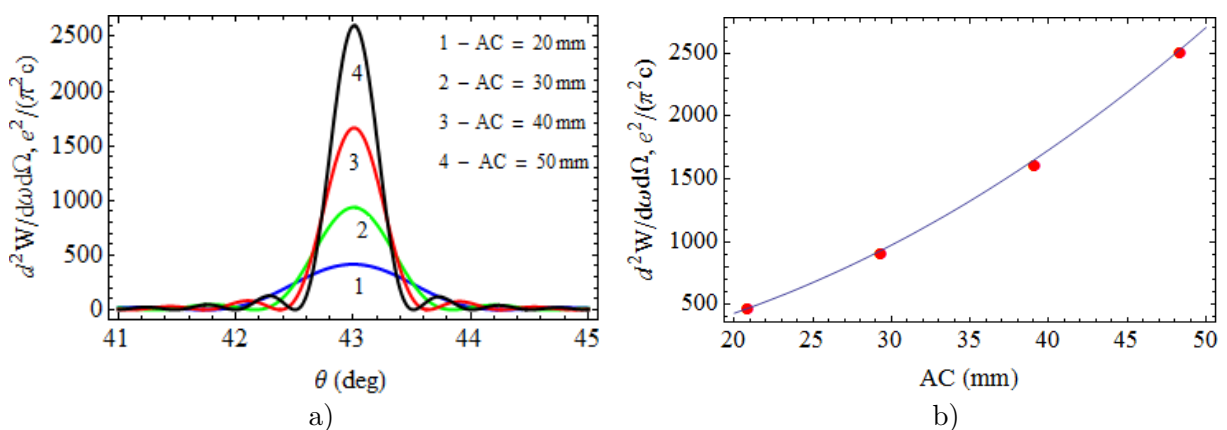


Figure 2. Angular distribution of the polarization radiation intensity for different AC side length (a-left). Dependence of the angular distribution maximum intensity versus AC side length (b-right). The calculation parameters are: $\varepsilon(\omega) = 1.9$ (PTFE); $\gamma = 97$; $\lambda = 0.3$ mm; $b = 5$ mm; $\alpha = 45^\circ$; $\varphi = 45^\circ$; $\phi = 0^\circ$.

The radiation intensity in the maximum of Cherenkov radiation distribution grows quadratically with increase of interaction length of the particle with the target as expected,

because the interaction surface increases. Increasing the AC side length from 20 mm to 50 mm we can significantly increase the photon yield.

The next step is to consider the intensity in maximum as a function of the impact parameter b . Figure 3 illustrates the dependences calculated for the same parameters as figure 2 and has the same color identities.

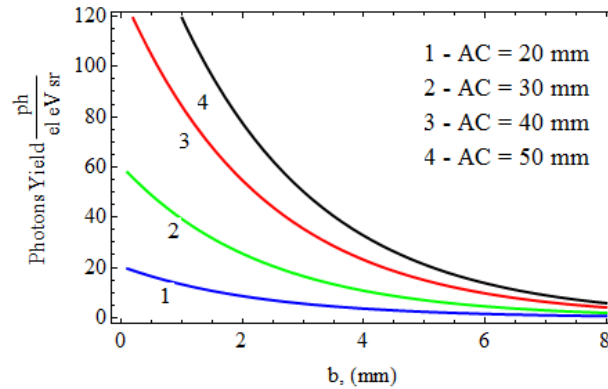


Figure 3. Dependences of ChR intensity in maximum as a function of the impact parameter calculated for different AC side lengths.

It is clear from the figure 3 that reducing the impact parameter the polarization radiation intensity increases exponentially for all AC side lengths. The analysis of the dependences enables us to choose an optimal impact parameter, will minimize the influence of the target on the beam and provide essential intensity.

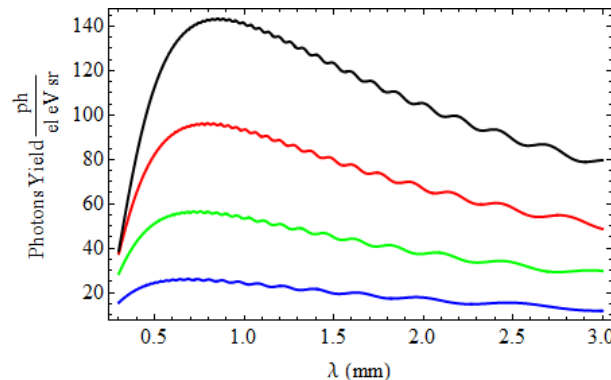


Figure 4. ChR spectra in angular distribution maximum calculated for different AC side lengths.

To evaluate the average photon yield per electron, we need to calculate the ChR photon spectrum using the equation (3). Figure 4 illustrates the calculation results in maximum of the angular distribution ($\theta_{Ch} = 43^\circ$) for the same parameters as previous figures. One may see that the maximum of the ChR photon yield is in the THz spectral range ($\lambda = 0.5 - 1$ mm).

Finally a number of CChR photons can be defined as

$$N = N_e^2 \int_{\Delta\omega} \frac{d\omega}{\hbar\omega} \exp \left[-2 \left(\frac{\omega}{\beta c \sigma_z} \right)^2 \right] \int_{\Delta\Omega} \frac{d^2W}{d\omega d\Omega} d\Omega, \quad (5)$$

where N_e is the number of electrons per bunch, $\hbar = h/2\pi$ is the reduced Planck constant. The exponential factor with the bunch length σ_z in the equation (5) is describe the longitudinal bunch form factor for the ChR [26].

Assuming 10^9 bunch population, 10^{-3} sr solid angle ($\Delta\theta = 0.5^\circ$ and $\Delta\phi = 10^\circ$ around the ChR maximum), 1 meV photon energy interval around maximum, and the AC side length of 50 mm, we have about 1.4×10^{14} photons per electron, corresponding to approximately 150 kW of peak power. Such a number of photons and the peak power are high enough to perform spectrometry experiments for chemical and biological samples. We intend to study the phenomenon spectral-angular characteristics and absolute power in order to propose the new radiator for the state of the art X-ray FELs as an auxiliary advantageous equipment.

3. Future plan and experimental setup

The experimental setup has been developed such that the direct interaction of the electron beam and the target can be controlled, and, if necessary, excluded. Non-invasive nature of the ChR gives an additional advantage as the beam parameters are kept almost the same as the initial ones. Therefore the beam can later be used by other experimental groups during the entire beam time. To realise the plan, we created an experimental setup schematically illustrated in the figure 5. Together with ChR the electron beam will generate forward DR, which will propagate along the electron beam trajectory but not in the direction of ChR.

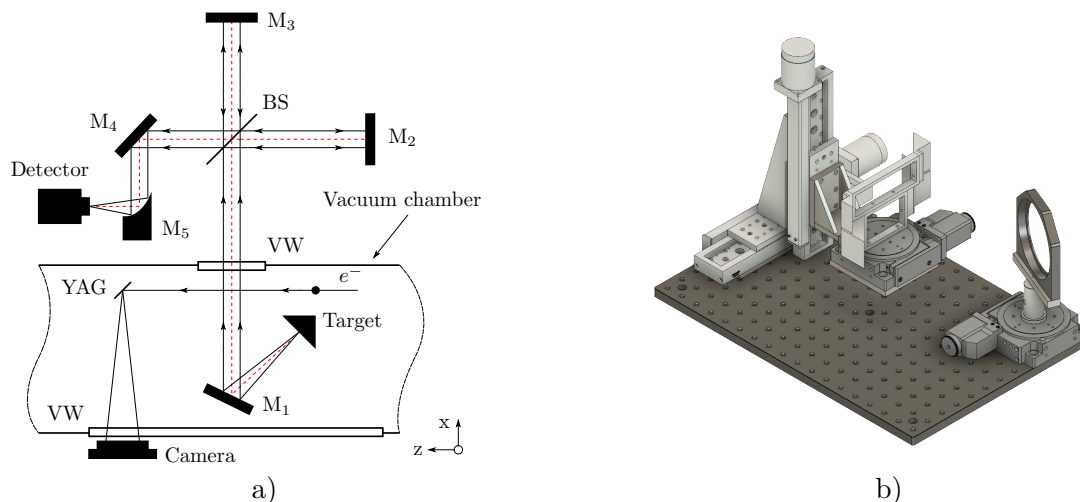


Figure 5. a) Principle scheme of the experiment; b) CAD drawing of the in-vacuum target and mirror M_1 manipulation system.

In the experiment we plan to use four different target with different AC side lengths to be able to compare the quadratic dependence of the ChR photon yield as a function of the interaction area with the theoretical predictions shown in the figure 2b. Geometrically all targets are the same, just the AC base length is 20, 30, 40, and 50 mm. The targets are mounted on a rotation/translation stage (see figure 5b) enabling to change the targets with respect to the beam. Horizontal translation also enables optimal impact parameter adjustment. A YAG screen placed downstream the target on a linear translation stage enables us to observe and optimise the electron beam shape and position. The image of the beam is observed in real time by the CCD camera installed outside the vacuum chamber. It shows the target position with respect to the beam.

The ChR induced by the electron beam Coulomb field propagates towards the rotating mirror M_1 and, then, which reflects the radiation out of the vacuum chamber through the fused silica vacuum window with the diameter of 150 mm. The mirror M_1 is mounted on the rotation stage allowing the angular distribution of the radiation to be scanned.

In order to measure the spectrum of the generated radiation the Michelson interferometer will be used. The interferometer consists of a stationary mirror M_2 , movable mirror M_3 and a beam

splitter BS . After the interferometer the radiation is directed by the mirror M_4 to the off-axis parabolic mirror M_5 which focuses the beam of radiation into the detector. A pyroelectric and Golay Cell detectors are used to detect the power of the radiation.

4. Conclusion

In the paper we have proposed an experiment on generation of intense THz radiation using non-invasive method based on ChR. We have presented the theoretical analysis of the ChR spectral-angular characteristics for the parameters of the CLARA facility being constructed at Daresbury Laboratory (UK). We have optimised the experimental conditions for the experiment, developed experimental hardware and prepared computer codes for future comparison with the experimental results.

Non-invasive nature of the ChR enables to put several radiator on the same beam to generate intense THz for several experiments in parallel. The spectral characteristics of the radiation will be applied for longitudinal bunch profile studies with femtosecond resolution when CLARA facility is commissioned.

Acknowledgments

The work was partly supported by the program “Nauka” of the Russian Ministry of Education and Science within the grant no. 3.709.2014/K, ADG-TX Leverhulme Trust Foundation International Network grant (no. IN-2015-012) and the Competitiveness Enhancement Program of Tomsk Polytechnic University. We would also like to acknowledge the Russian Foundation for Basic Research (grant no. 14-02-31642-mol_a).

References

- [1] Siegel P H 2002 *IEEE Trans. on Microwave Theory and Techniques* **50** 910
- [2] Smye S W, Chamberlain J M, Fitzgerald A J and Berry E 2001 *Physics in Medicine and Biology* **46** R101
- [3] Kampfrath T, Tanaka K and Nelson K A 2013 *Nature Photonics* **7** 680
- [4] Dudovich N, Oron D and Silberberg Y 2002 *Nature* **418** 512
- [5] Van der Weide D 2003 *Opt. Photonics News* **14** 48
- [6] Gorshunov B, Volkov A, Spektor I, Prokhorov A *et al* 2005 *Int. J. of Infrared and Millimeter Waves* **26** 1217
- [7] Vergheze S, McIntosh K A, and Brown E R 1997 *IEEE Trans. Microwave Theory Tech* **45** 1301
- [8] Matsuura S, Blake G A, Wyss R A, Pearson J C *et al* 1999 *Appl. Phys. Lett.* **74** 2872
- [9] LCLS Technical Design Report 2002 (*SLAC*) R-593 <http://www-ssrl.slac.stanford.edu/lcls/cdr/>
- [10] XFEL Technical Design Report 2006 (*DESY*) 097 <http://xfel.desy.de>
- [11] Ryazanov M I and Tilinin I S 1976 *Sov. Phys. – JETP* **44** 1092
- [12] Karataev P, Araki S, Hamatsu R, Hayano H *et al* 2004 *Phys. Rev. Lett.* **93** 244802
- [13] McMillan E M 1945 *Phys. Rev.* **68** 144
- [14] Bolotovskii B M and Galstyan E A 2000 *Phys.-Usp.* **43** 755
- [15] Jelley J V 1958 *Čerenkov radiation and its applications* (London: Pergamon Press) p 331
- [16] Karlovets D V and Potylitsyn A P 2009 *JETP Lett.* **90** 368
- [17] Karlovets D V 2011 *J. Exp. Theor. Phys.* **113** 27
- [18] Kruchinin K O and Karlovets D V 2012 *Russ. Phys. J.* **55** 9
- [19] Shevelev M V and Konkov A S 2014 *J. Exp. Theor. Phys.* **118** 501
- [20] Shevelev M V, Konkov A S and Aryshev A S 2015 *Phys. Rev. A* **92** 053851
- [21] Naumenko G A, Potylitsyn A P, Shevelev M V and Popov Y A 2011 *JETP Lett.* **94** 258
- [22] Shevelev M, Naumenko G, Potylitsyn A and Popov Yu 2012 *J. Phys: Conf. Ser.* **357** 012020
- [23] Naumenko G, Potylitsyn A, Shevelev M, Bleko V *et al* 2014 *J. Phys: Conf. Ser.* **517** 012004
- [24] Bleko V V, Konkov A S and Soboleva V V 2015 *Nucl. Instrum. Methods B* **355** 129
- [25] CLARA Conceptual Design Report 2013 (*STFC*) <http://www.stfc.ac.uk/files/science-publications/clara-conceptual-design-report-2013/>
- [26] Naumenko G A 2015 *Adv. Mat. Res.* **1084** 138